

Back interface passivation for ultrathin Cu(In,Ga)Se_2 solar cells with Schottky back contact: A trade-off of electrical effects

Ye Tu(涂野), Yong Li(李勇), and Guanchao Yin(殷官超)
Citation: Chin. Phys. B, 2023, 32 (**6**): 068101. DOI: 10.1088/1674-1056/acc05b
Journal homepage: http://cpb.iphy.ac.cn; http://iopscience.iop.org/cpb

What follows is a list of articles you may be interested in

Influence of the lattice parameter of the AlN buffer layer on the stress state of GaN film grown on (111) Si

Zhen-Zhuo Zhang(张臻琢), Jing Yang(杨静), De-Gang Zhao(赵德刚), Feng Liang(梁锋), Ping Chen(陈平), and Zong-Shun Liu(刘宗顺)
Chin. Phys. B, 2023, 32 (**2**): 028101. DOI: 10.1088/1674-1056/ac6b2b

Bottom-up approaches to microLEDs emitting red, green and blue light based on GaN nanowires and relaxed InGaN platelets

Zhaoxia Bi(毕朝霞), Anders Gustafsson, and Lars Samuelson
Chin. Phys. B, 2023, 32 (**1**): 018103. DOI: 10.1088/1674-1056/aca9c2

Degradation mechanisms for a-InGaZnO thin-film transistors functioning under simultaneous DC gate and drain biases

Tianyuan Song(宋天源), Dongli Zhang(张冬利), Mingxiang Wang(王明湘), and Qi Shan(单奇)
Chin. Phys. B, 2022, 31 (**8**): 088101. DOI: 10.1088/1674-1056/ac673e

Effects of electrical stress on the characteristics and defect behaviors in GaN-based near-ultraviolet light emitting diodes

Ying-Zhe Wang(王颖哲), Mao-Sen Wang(王茂森), Ning Hua(化宁), Kai Chen(陈凯), Zhi-Min He(何志敏), Xue-Feng Zheng(郑雪峰), Pei-Xian Li(李培咸), Xiao-Hua Ma(马晓华), Li-Xin Guo(郭立新), and Yue Hao(郝跃)
Chin. Phys. B, 2022, 31 (**6**): 068101. DOI: 10.1088/1674-1056/ac4cb8

Suppression of electron and hole overflow in GaN-based near-ultraviolet laser diodes

Yao Xing(邢瑶), De-Gang Zhao(赵德刚), De-Sheng Jiang(江德生), Xiang Li(李翔), Zong-Shun Liu(刘宗顺), Jian-Jun Zhu(朱建军), Ping Chen(陈平), Jing Yang(杨静), Wei Liu(刘炜), Feng Liang(梁锋), Shuang-Tao Liu(刘双韬), Li-Qun Zhang(张立群), Wen-Jie Wang(王文杰), Mo Li(李沫), Yuan-Tao Zhang(张源涛), Guo-Tong Du(杜国同)
Chin. Phys. B, 2018, 27 (**2**): 028101. DOI: 10.1088/1674-1056/27/2/028101

Back interface passivation for ultrathin Cu(In,Ga)Se_2 solar cells with Schottky back contact: A trade-off of electrical effects

Ye Tu(涂野)[1], Yong Li(李勇)[2], and Guanchao Yin(殷官超)[1,†]

[1] *School of Materials Science and Engineering, Wuhan University of Technology, Wuhan* 430070, *China*
[2] *Faculty of Physics, University of Duisburg-Essen and CENIDE, Forsthausweg* 2, *D*-47057 *Duisburg, Germany*

(Received 29 November 2022; revised manuscript received 25 January 2023; accepted manuscript online 2 March 2023)

Back interface passivation reduces the back recombination of photogenerated electrons, whereas aggravates the blocking of hole transport towards back contact, which complicate the back interface engineering for ultrathin CIGSe solar cells with a Schottky back contact. In this work, theoretical explorations were conducted to study how the two contradictory electrical effects impact cell performance. For ultrathin CIGSe solar cells with a pronounced Schottky potential barrier ($E_h > 0.2$ eV), back interface passivation produces diverse performance evolution trends, which are highly dependent on cell structures and properties. Since a back Ga grading can screen the effect of reduced recombination of photogenerated electrons from back interface passivation, the hole blocking effect predominates and back interface passivation is not desirable. However, when the back Schottky diode merges with the main pn junction due to a reduced absorber thickness, the back potential barrier and the hole blocking effect is much reduced on this occasion. Consequently, cells exhibit the same efficiency evolution trend as ones with an Ohmic contact, where back interface passivation is always advantageous. The discoveries imply the complexity of back interface passivation and provide guidance to manipulate back interface for ultrathin CIGSe solar on TCOs with a pronounced Schottky back contact.

Keywords: ultrathin cigse solar cells, Schottky back contact, back interface passivation, back recombination, hole blocking

PACS: 81.05.Ea, 73.30.+y, 73.40.Mr **DOI:** 10.1088/1674-1056/acc05b

1. Introduction

Ultrathin Cu(In,Ga)Se_2 (CIGSe) solar cells, namely with a sub-500-nm thick absorber, have been attracting great attention.[1–5] Compared to conventional cells with an absorber thickness beyond 2 μm, ultrathin CIGSe solar cells reduce the absorber material consumption to a great extent, simultaneously relaxing the concern of indium scarcity and lowering the manufacturing cost in mass production.[6,7] Additionally, ultrathin absorbers enhance the tolerance for their fabrication conditions (*e.g.* lower substrate temperature, non-vacuum) since they permit a shorter minority diffusion length, which can further reduce the manufacturing.[8–11] However, their efficiencies are heavily restrained with a loss of more than 6% (abs.) than their thick counterparts. Two issues of back recombination and insufficient light absorption are jointly responsible for the poor PV performance.[1–4,12]

Back recombination specifically points to photogenerated minorities (electrons) recombining at the back interface of CIGSe/back contact.[3,11,12] It is extraordinarily severe for ultrathin absorbers because they generate a high density of photogenerated carriers close to back interface, which are more liable to transport to back interface and recombine there. Optically, ultrathin CIGSe solar cells cannot completely absorb the incident light after the first pass, especially in the long wavelengths. Moreover, the common CIGSe/Mo back interface exhibits a quite poor optical reflectivity and the unabsorbed light after the first pass will be dissipated by Mo rather than being reflected back into absorbers for the second propagation.[5,13,14] To address the two challenges, point-contact structures, composed of dielectric thin films with local openings for carrier collection, were widely employed to passivate back interface.[15–22] They can greatly reduce the back recombination by lowering the interface recombination velocity S_b as well as enhance absorption by improving the back reflectivity of CIGSe/Mo.

Besides on opaque Mo, TCOs (transparent conductive oxides) are an alternative for back contact.[23–25] They are able to avoid the parasitic absorption of Mo and permits the unabsorbed light after the first pass propagating out of ultrathin cells.[26,27] This unique feature offers ultrathin CIGSe solar cells on TCOs a promising application potential in solar windows,[28,29] bifacial application,[30,31] and top cells in tandem configuration.[32] However, due to the mismatch of work functions between absorbers and TCOs, CIGSe solar cells on TCOs exhibit a Schottky back contact with a potential barrier, which thus forms an opposed back diode to the main pn junction.[24,33,34] The Schottky back diode is able to hinder the transport of holes towards TCO back contact, which mainly impair open circuit voltage (V_{oc}) and fill factor (FF).[35] Additionally, it was both theoretically[36] and experimentally[37] discovered that passivating back interface (lowering back re-

†Corresponding author. E-mail: guanchao.yin@whut.edu.cn
© 2023 Chinese Physical Society and IOP Publishing Ltd

combination velocity S_b) will further aggravate the hole blocking effect. The underlying mechanism is that the hole transport towards TCO back contact can be assisted through their recombination at back interface, a lower S_b thus points to an anabatic hole blocking effect.[25]

Consequently, it is inferred that back interface passivation induces two contradictory electrical effects for ultrathin CIGSe solar cells with a Schottky back contact. It brings the beneficial reduction of photogenerated electrons at back interface,[15–22] simultaneously aggravates the harmful hole blocking effect.[36] It should be noted that, despite of a relatively low potential barrier ($E_h < 0.2$ eV) and being typically treated as an Ohmic contact, CIGSe/Mo is indeed a Schottky back contact.[38,39] This indicates that the contradictory electrical effects should be both available for cells on Mo and TCOs. Previous experimental study revealed that back passivation contributed to performance enhancement for ultrathin cells on Mo without exception.[19,21] Whereas, both performance improvement and deterioration were experimentally observed after back interface passivation for cells on TCOs, which is not clarified yet.[25,40] This indicates that contradictory electrical effects from back interface passivation are complicated and further explorations are required, especially for cells with a pronounced Schottky back contact.

In this work, we employ 1D software SCAPS[41] and conduct theoretical investigations on how back interface passivation affects ultrathin CIGSe solar cells with a Schottky back contact. Firstly, the contradictory electrical effects arising from back interface passivation will be identified individually and then their joint effects on cell performance are extensively explored. Due to the trade-off of the two contradictory electrical effects, ultrathin CIGSe solar cells with a pronounced Schottky back contact ($E_h > 0.2$ eV) produce diverse efficiency-S_b vibration tendencies, which is highly dependent on cell structures and properties. This poses a sharp contrast to ones with an $E_h < 0.2$ eV, where a passivated back interface is always desired. The findings will deepen the understanding of back interface passivation and provide theoretical guidance to manipulate back interface for an optimum performance of ultrathin CIGSe solar cells on TCOs.

2. Simulation

2.1. Electrical model

Electrical simulations are performed employing the one-dimensional (1D) software SCAPS,[41] which offers great convenience to adjust S_b and E_h. As illustrated in Fig. 1, CIGSe solar cells have a typical structure of AZO(Al:ZnO)/i-ZnO/CdS/CIGSe/back contact. AZO/i-ZnO/CdS have a constant thickness of 240 nm/130 nm/50 nm, which follow experimental samples fabricated from the standard procedure in Helmholtz Zentrum Berlin.[42,43] A flat bandgap is simply configured for the absorber if absent of special instructions in this work. At interfaces a small spike from CIGSe to CdS and a cliff from CdS to ZnO are assumed. Mid-gap neutral defects are introduced to adjust the carrier lifetime in both layers and interfaces. The fermi level at the interface of CdS/CIGSe is pinned by shallow donor defects and then an inversion for CdS/CIGSe interface is obtained.[44,45] Table 1 lists relevant electrical parameters of each layer and

Table 1. Device parameters of simulated CIGSe solar cells. In the table, ΔE_c: conduction band offset, E_g: band gap, $\varepsilon/\varepsilon_0$: relative permittivity, d: layer thickness, χ: affinity, μ_e and μ_h: electron and hole mobilities, V_e and V_h: velocities of electrons and holes, E_g (in unit eV): band gap energy, N_c and N_v: effective densities of states in conduction band and valence band, σ_e and σ_h: capture cross-sections of electrons and holes.

Parameter	CIGSe	CdS	ZnO	AZO
d (nm)	variable	50	130	240
E_g (eV)	1.2	2.42	3.3	3.3
χ (eV)	4.5	4.4	4.6	4.5
$\varepsilon/\varepsilon_0$	13.6	10	10	10
N_c (cm^{-3})	2×10^{18}	4×10^{18}	4×10^{18}	1×10^{19}
N_v (cm^{-3})	1×10^{19}	1×10^{19}	1×10^{19}	1×10^{19}
V_e (cm/s)	1×10^{7}	1×10^{7}	1×10^{7}	1×10^{7}
V_h (cm/s)	1×10^{7}	1×10^{7}	1×10^{7}	1×10^{7}
μ_e (cm^2/V·s)	100	100	100	50
μ_h (cm^2/V·s)	20	20	20	50
$N_{D/A}$ (cm^{-3})	1×10^{16}	1×10^{15}	1×10^{18}	1×10^{20}
Bulk defect properties				
N (cm^{-2})	5×10^{15}	1×10^{17}	1×10^{19}	1×10^{20}
σ_e (cm^2)	1×10^{-14}	5×10^{-17}	1×10^{-18}	1×10^{-15}
σ_h (cm^2)	1×10^{-16}	1×10^{-13}	1×10^{-15}	1×10^{-15}
Interface properties				
	CIGSe/CdS[1]	CIGSe/CdS[2]	CdS/ZnO	ZnO/AZO
ΔE_c (eV)	1.1	0.6	1.21	1.2
N (cm^{-2})	1×10^{12}	1×10^{12}	1×10^{12}	1×10^{12}
σ_e (cm^2)	1×10^{-13}	1×10^{-13}	1×10^{-13}	1×10^{-13}
σ_h (cm^2)	1×10^{-13}	1×10^{-13}	1×10^{-13}	1×10^{-13}

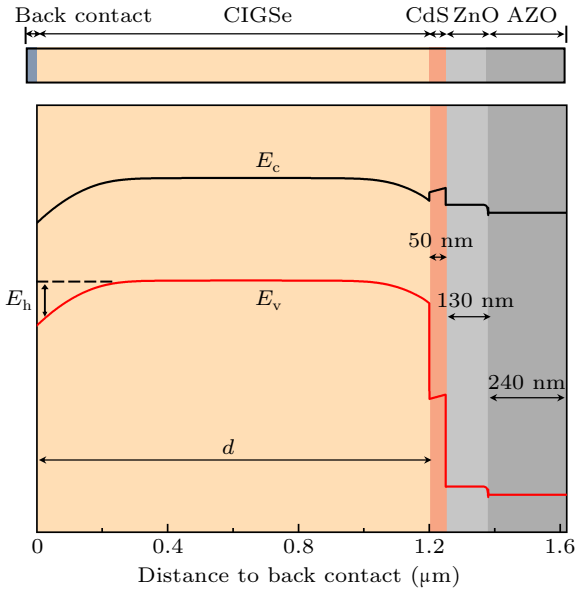


Fig. 1. The sketch of the band diagram of the CIGSe solar cells (AZO/ZnO/CdS/CIGSe/back contact) with a back potential barrier E_h. E_c and E_v are conduction and valence band edges, respectively.

interface, and the resultant band diagram (absorber thickness $d = 1200$ nm, $E_h = 0.4$ eV) is also presented in Fig. 1. S_b (assumed the same for electrons and holes) ranges from 10^3 cm/s to 10^7 cm/s and E_h (Schottky barrier height for holes, with respect to the equilibrium valence band[36,40,44]) from 0 eV to 0.5 eV.

2.2. Optical model

Since the built-in optical model in SCAPS is quite simple without considering the multiple reflections at interfaces, this may result in non-negligible error for the local generation of photogenerated carriers, especially close to back interface. To make the electrical simulation results more liable and realistic, generation profiles of photogenerated carriers are obtained from optical simulations based on finite element method (FEM) and then introduced into SCAPS for electrical simulations. The optical structure settings are exactly the same as ones in SCAPS. Back contact is set 200-nm thick. Optical constants of each layer were extracted from experimental samples[46] and interfaces are assumed flat.

For optical simulations, electric field intensity E in the device is obtained at an AM 1.5 illumination condition. We defined $\psi(x,\lambda)$ as absorbed light energy, which is a function of position x and wavelength λ

$$\psi(x,\lambda) = \frac{1}{2}\varepsilon_0 c\alpha n|E|^2, \tag{1}$$

where ε_0 is the vacuum dielectric constant, c is the light speed, α is the absorption coefficient formulated by $\alpha = 4\pi k/\lambda$ (k is the extinction coefficient), and n is the index of refraction.

Then, $\psi(x,\lambda)$ is integrated in the wavelength range from 350 nm to 1200 nm, the generation rate $G(x)$ is finally expressed by

$$G(x) = \frac{1}{hc}\int_{350}^{1200} \lambda\,\psi(x,\lambda)\,\mathrm{d}\lambda, \tag{2}$$

where h is Planck constant.

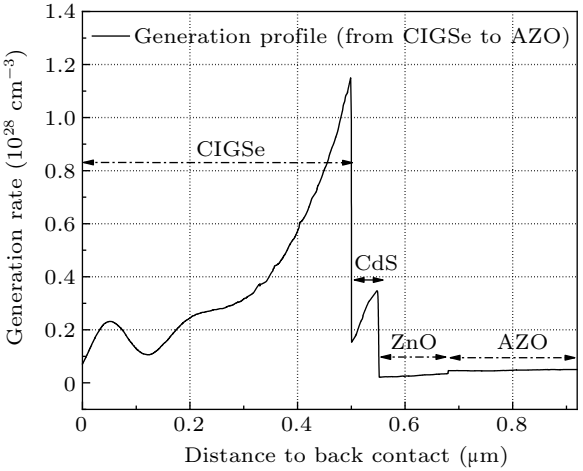


Fig. 2. Generation profile of photogenerated carriers for ultrathin CIGSe solar cells on Mo ($d = 500$ nm).

Figure 2 plots the calculated generation profile of ultrathin CIGSe solar cells on Mo ($d = 500$ nm) as an example. Fluctuations can be spotted in the vicinity of back interface due to the wave interferences, which will be not available from the built-in optical model in SCAPS.

3. Result and discussion

3.1. Electrical effects

We start from an ultrathin cell ($d = 500$ nm) with an Ohmic back contact ($E_h = 0$ eV). Figure 3(a) shows dark J_{dark}–V and light J_{light}–V curves as a function of S_b. As S_b reduces, the photovoltaic performance exhibits an improvement, which agrees well with previous investigations.[13–21] This is attributed to the reduced back recombination of photogenerated electrons arising from back interface passivation. However, this positive effect was mainly reflected by the enhancement of short-circuit current density (J_{sc}) in prior study[19,21,22] and lacks of direct evidence how the reduced back recombination of photogenerated electrons improves V_{oc} and FF. According to the basic equation ($J_{light} = J_{photo} - J_{dark}$) for one-diode solar cells, J_{light} is determined by J_{photo} (the current density out of photogenerated carriers) and J_{dark}. Thus, J_{photo}–V curves can be calculated and are also attached in Fig. 3(a). It can be observed that J_{photo} is reducing as the bias voltage is increasing for a single J_{photo}–V curve. This is because that the space charge region (SCR) is more compensated as the bias voltage increases, more photogenerated carriers are located out of SCR and are liable to recombine at back interface. Additionally, among J_{photo}–V curves, a lower S_b corresponds to a higher J_{photo} covering the whole bias range of interest and a smaller slope. This visually explains that the reduced back recombination of photogenerated electrons not only improves J_{sc}, but also V_{oc} and FF. Other than experimental characterizations, SCAPS can also readily offer the recombination current density of photogenerated minorities. Figure 3(b) plots the recombination current density of phogenerated electrons at back interface ($J_{back\text{-}interf}$) and in bulk (J_{bulk}). $J_{back\text{-}interf}$ shows a pronounced decrease as S_b decreases, whereas J_{bulk} hardly changes. This provides solid evidence that back interface passivation reduces the recombination of photogenerated electrons indeed at back interface. Remarkably, another positive effect out of back interface passivation is spotted in J_{dark}–V curves. A lower S_b produces a lower J_{dark} when the bias is approaching to V_{oc}. Dark current is a recombination current and a smaller S_b thereby decreases J_{dark}. Based on the basic equation for one-diode solar cells stated above, a deceased J_{dark} contributes to cell performance as well. To our best knowledge, this beneficial effect out of back interface passivation is discovered for the first time. Nevertheless, judging

from Fig. 3(a), the S_b dependent evolution magnitude is quite moderate for J_{dark} compared to J_{photo}. This is probably why this positive effect was not experimentally distinguished before. Therefore, the reduced recombination of photogenerated electrons from back interface passivation is only considered as the positive effect in the following.

Since photogenerated carriers close to back interface is marginal, back interface passivation barely reduces back recombination of photogenerated electrons for conventional CIGSe solar cells with an absorber thickness beyond 2 μm. To exclude the effect of reduced back recombination of photogenerated carriers, we set a thick CIGSe solar cell ($d = 2000$ nm) to purely explore the hole blocking effect from back interface passivation for CIGSe solar cells with a Schottky back contact. Figure 4 shows J_{light}–V curves at an $E_h = 0.3$ eV as a function of S_b. Compared to the cell with an Ohmic contact (also attached in Fig. 4, dash–dotted line), there exists an apparent J_{light} loss in the fourth quadrant and a suppression for the forward current in the first quadrant. As a result, V_{oc} and FF are largely reduced. More notably, the J_{light} loss and the suppression of forward current are increasingly aggravated with the decrease of S_b. Our recent study has identified that the hole transport towards back contact can be assisted via their recombination at back interface.[36] Thereby, a lower S_b thereby corresponds to a severer hole blocking effect, which is detrimental to cell performance.

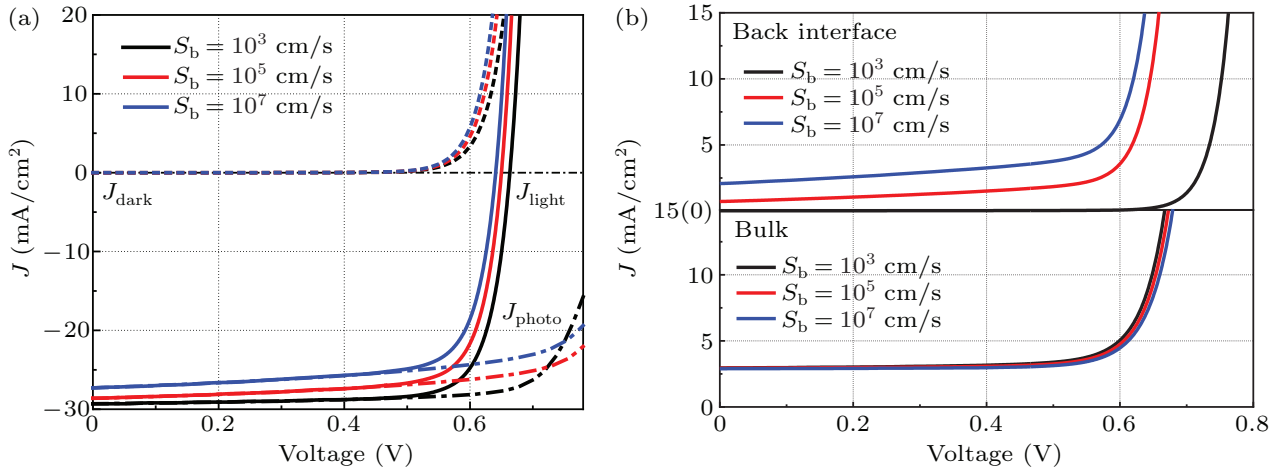


Fig. 3. The J–V curves of CIGSe solar cells for (a) J_{light}, J_{dark}, and J_{photo}; (b) recombination current density of phogenerated electrons at back interface ($J_{back\text{-}interf}$) and in the bulk (J_{bulk}).

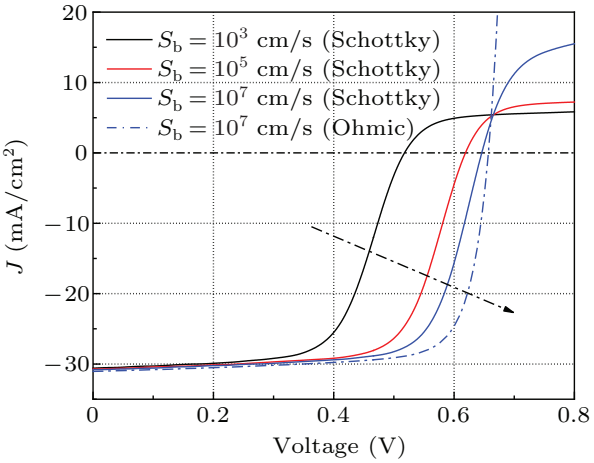


Fig. 4. The J_{light}–V curves of thick CIGSe solar cells ($d = 2000$ nm) with a Schottky potential barrier (E_h =0.3 eV) as a function of back recombination velocity S_b.

To explore the combined action of the two contradictory effects for ultrathin CIGSe solar cells with a Schottky back contact, figure 5(a) plots J_{light}–V curves of ultrathin CIGSe solar cells ($d = 500$ nm) at an $E_h = 0.4$ eV. The J_{sc} increase proves the presence of the positive effect of reduced recombination of photogenerated electrons. However, a reduced S_b is overall harmful for ultrathin CIGSe solar cells, despite with an increased J_{sc}. This implies that the detrimental hole blocking effect exists and surpasses the positive recombination reduction of photogenerated electrons. To identify the dependence of cell performance on S_b, figure 5(b) further shows the efficiency contour as a function of S_b and E_h. Due to the absence of the detrimental hole blocking effect, ultrathin cells with an Ohmic contact ($E_h = 0$ eV) exhibit a better performance than those with a Schottky contact and the efficiency is monotonically increasing as S_b is reducing. When $E_h = 0.1$ eV, the efficiency follows a similar trend as the case of $E_h = 0$ eV. For $E_h \geq 0.2$ eV, the hole blocking effect is not non-negligible and the efficiency–S_b evolution differs a lot. The efficiencies are firstly decreasing as S_b evolves from 10^7 cm/s to 10^4 cm/s and then improving when S_b further decreases to 10^3 cm/s, leading to the lowest efficiency value at the S_b of 10^4 cm/s. This illustrates that the two contradictory electrical effects are competing as a function S_b. The hole blocking effect dominates at relatively high S_b ranges. However, when S_b evolves from 10^4 cm/s to 10^3 cm/s, the reduced back recombination of photogenerated electrons starts to play a dominant role. This can be reflected by the enhancement magnitude of J_{sc} as shown in

Fig. 5(a), where J_{sc} increases sharply when S_b reduces from 10^4 cm/s to 10^3 cm/s. Because CIGSe solar cells on Mo are typically reported to have an $E_h < 0.2$ eV[38,39] and the resultant hole blocking effect is modest, inserting dielectric point-contact structures at back interface always contributes to performance enhancement.[17–22] The theoretical results here are quite consistent with the experimental observations, where a passivated back interface is beneficial when $E_h < 0.2$ eV.

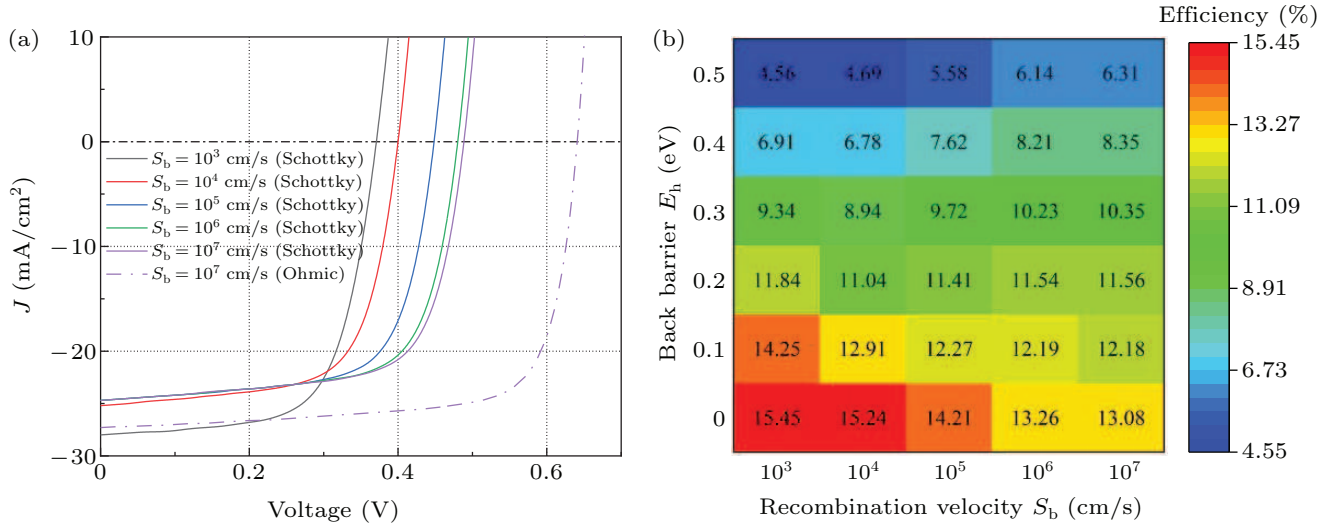


Fig. 5. (a) The J_{light}–V curves at an $E_h = 0.4$ eV, and (b) efficiency contour as a function of S_b and E_h for ultrathin CIGSe solar cells ($d = 500$ nm).

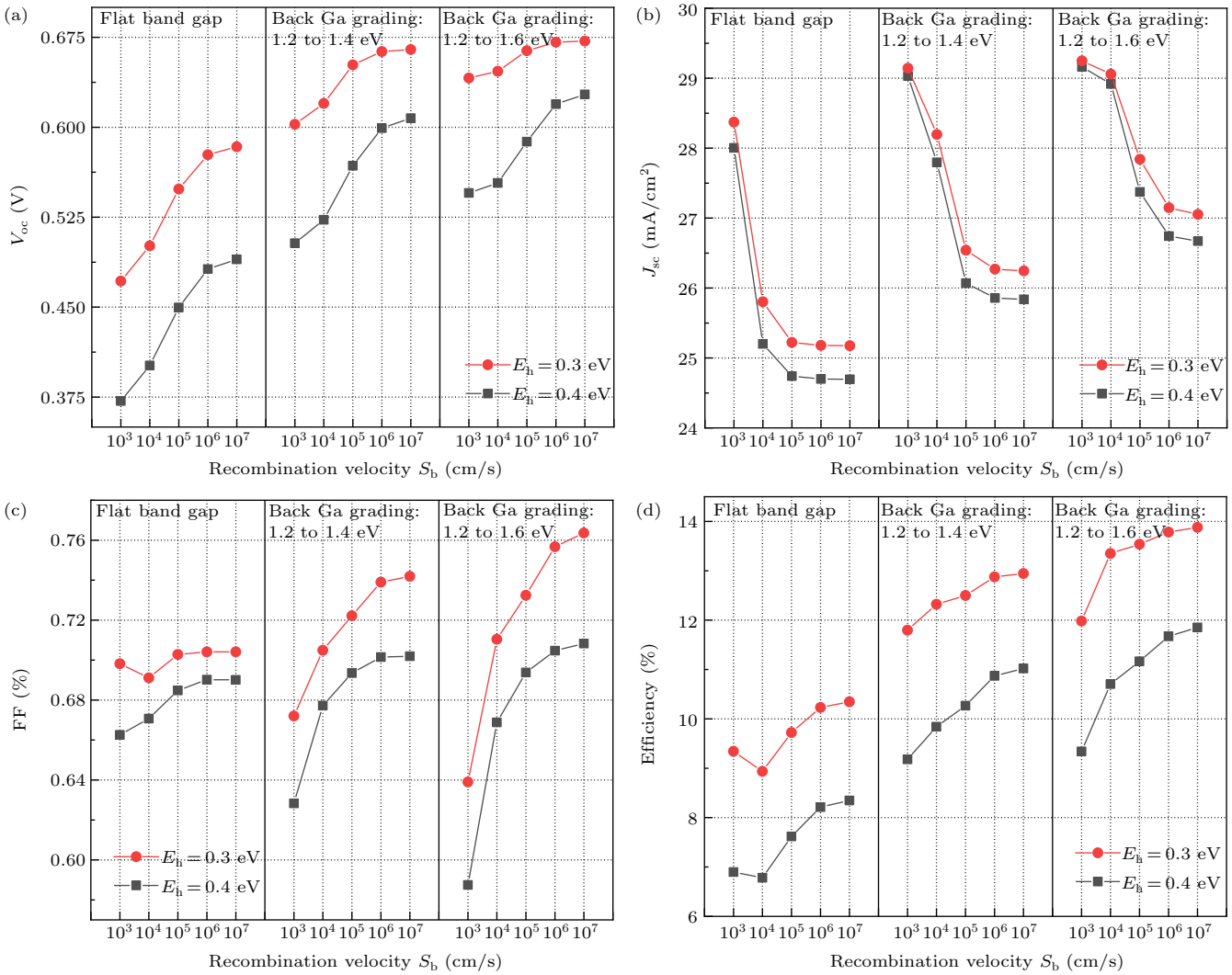


Fig. 6. The J_{light}–V parameters of ultrathin CIGSe solar cells ($d = 500$ nm) with a Schottky back contact ($E_h = 0.3$ eV and 0.4 eV) for various back Ga gradings, (a) V_{oc}, (b) J_{sc}, (c) FF, and (d) efficiency.

3.2. Effects of back Ga grading and absorber thickness

From the analysis above, the performance evolution on back interface passivation relies on the trade-off of the two contradictory electrical effects for ultrathin CIGSe solar cells with an $E_h > 0.2$ eV. This means that any structure or property, which can influence the degree of the two electrical effects, may alter the efficiency–S_b dependence. Back Ga grading and absorber thickness are the two parameters which vary a lot among experimental cells. Therefore, in the following, we will emphasize on exploring how the back Ga grading and absorber thickness impact the two electrical effects and the resultant efficiency–S_b dependence.

To create a back Ga grading for absorbers, the 500-nm thick CIGSe layer is arbitrarily divided into two sub-absorbers. The one close to CdS maintains a constant bandgap of 1.2 eV and a thickness of 50 nm, the other one is configured with a linear bandgap towards back contact from 1.2 eV to 1.4 eV (or 1.6 eV) by increasing the conduction band. Figure 6 compares J_{light}–V parameters of ultrathin CIGSe solar cells with various back Ga gradings. Since it can reduce the back recombination of photogenerated electrons, the back Ga grading overall enhances the performance to a great extent. The higher the back Ga grading, the greater the performance. Further, the back Ga grading simplifies the effiency–S_b evolution trend, where cells with the back Ga grading show a monotonously decreasing efficiency as S_b is reducing. This is significantly different from the flat bandgap cells with a minimum cell performance at $S_b = 10^4$ cm/s as shown in Fig. 5(b).

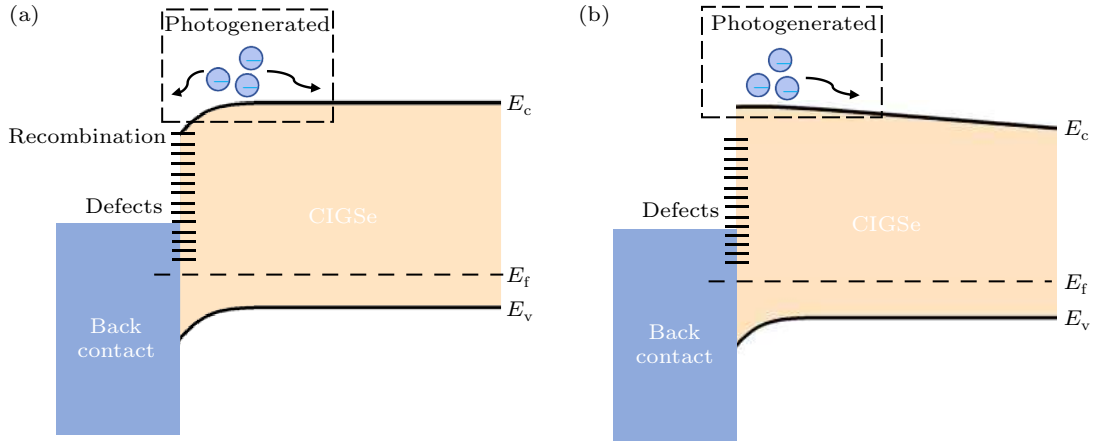


Fig. 7. Schematic band diagrams of ultrathin CIGSe solar cell ($d = 500$ nm) with a Schottky back contact for (a) a flat bandgap and (b) a back Ga grading.

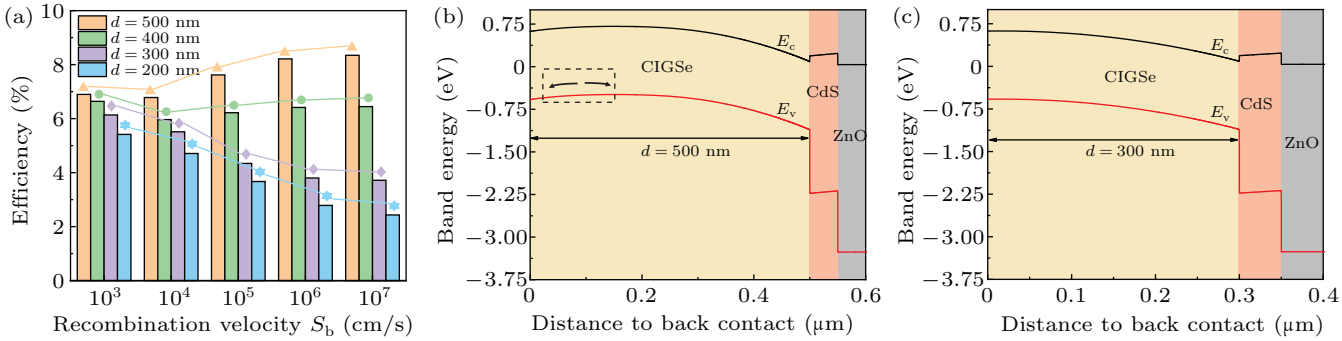


Fig. 8. (a) Efficiency–S_b histogram and [(b), (c)] band diagrams of ultrathin CIGSe solar cells with a Schottky back contact ($E_h = 0.4$ eV) at various absorber thicknesses: (b) $d = 500$ nm, (c) $d = 300$ nm.

It should be specially stressed that, in contrast to ultrathin cells with an Ohmic contact, the Schottky back potential further exacerbates the back recombination of photogenerated electrons. As illustrated in Fig. 7(a), the back Schottky potential results in a bending of conduction band toward back contact and will drift photogenerated electrons towards back interface. Fortunately, a back Ga grading is able to compensate the bending of conduction band (see Fig. 7(b)) and this will greatly reduce the back recombination of photogenerated electrons. Exactly because of this, back interface passivation will exert a reduced influence on restraining the back recombination of photogenerated electrons. Consequently, as S_b reduces, the increased hole blocking effect weights over the reduced back recombination of photogenerated electrons and cell performance monotonously deteriorates.

Figure 8(a) plots absorber thickness-dependent efficiency–S_b histograms of ultrathin cells with a $E_h = 0.4$ eV. Unlike cells with an absorber thickness of 400 nm and 500 nm, cells with 200-nm absorber or 300-nm absorber exhibit a third efficiency–S_b evolution trend. The efficiency is monotonously

improving as S_b is reducing, completely opposite to the evolution trend for cells with a back Ga grading demonstrated in Fig. 6. To identify the underlying reason, figures 8(b)–8(c) illustrate the sketches of band diagrams for $d = 500$ nm and 300 nm at a bias of zero, respectively. At $d = 500$ nm, an obvious back diode out of the Schottky potential is present close to back contact, which is opposed to the main pn junction in polarity. Interestingly, for $d = 300$ nm, the back diode disappears and only one diode with the same polarity to the main pn one is available. This is due to that the two space charge regions overlap and the back diode merges with the main pn junction when the absorber is thin enough. The mergence inhibits the hole blocking effect and the positive effect (reduced recombination of photogenerated electrons) dominates. Therefore, back interface passivation contributes to performance enhancement, producing a similar efficiency–S_b trend to cells with $E_h < 0.2$ eV.

3.3. Implication for ultrathin CIGSe solar cells on TCO back contacts

Ultrathin CIGSe solar cells on TCOs have a pronounced Schottky back contact.[25–27,31,35] Back interface passivation therefore not only brings the positive recombination reduction of photogenerated electrons, but also exacerbates the harmful hole blocking effect. Various efficiency–S_b evolution trends are demonstrated above, which depend on the trade-off of the two contradictory electrical effects. Since a back Ga grading is experimentally present in most cases, back interface passivation may be not desirable for ultrathin CIGSe solar cells on TCOs. To the contrary, introducing a high density of defect states at back interface is preferred in this case. However, when the absorber thickness is thin enough that the main pn junction and the back Schottky diode deeply merge, back interface passivation turns to be beneficial. This suggests, unlike cells on Mo with $E_h < 0.2$ eV, back interface passivation is complicated for ultrathin cells on TCOs. Here only back Ga grading and absorber thickness are explored, but in principle, any structure or property which may alter the weight of the two contradictory electrical effects will impact the integral effect of back interface passivation.

4. Conclusion

In this work, the reduced back recombination of photogenerated electrons and the aggravated hole blocking effect, both arising from back interface passivation, were identified individually. Their competing effects with respect to cell performance were extensively explored for ultrathin CIGSe solar cells with a pronounced Schottky back contact ($E_h > 0.2$ eV). The efficiency–S_b evolution trends are highly dependent on cell structures and properties. A back Ga grading enables to shield the reduced back recombination arising from back interface passivation and the hole blocking effect therefore dominates. This results in a monotonous performance deterioration after back interface passivation, indicating that back interface passivation at this case is not favorable. Remarkably, when the absorber thickness is thin enough that the Schottky diode merges with the main pn junction, the hole blocking effect is restrained and cells exhibit a similar efficiency–S_b evolution trend as ones with an Ohmic contact, where back interface passivation is desirable. Those findings verify the complexity of back interface passivation for ultrathin CIGSe solar and may point to completely different optimization paths for ultrathin CIGSe cells on TCOs.

Acknowledgment

Project supported by the National Natural Science Foundation of China (Grant No. 51802240).

References

[1] Lundberg O, Bodegard M, Malmstrom J and Stolt L 2003 *Progress in Photovoltaics* **11** 77
[2] Gloeckler M and Sites J R 2005 *J. Appl. Phys.* **98** 103703
[3] Bouttemy M, Tran-Van P, Gerard I, Hildebrandt T, Causier A, Pelouard J L, Dagher G, Jehl Z, Naghavi N, Voorwinden G, Dimmler B, Powalla M, Guillemoles J F, Lincot D and Etcheberry A 2011 *Thin Solid Films* **519** 7207
[4] Kaelin M, Rudmann D and Tiwari A N 2004 *Solar Energy* **77** 749
[5] Vermang B, Watjen J T, Fjallstrom V, Rostvall F, Edoff M, Kotipalli R, Henry F and Flandre D 2014 *Progress in Photovoltaics* **22** 1023
[6] Tao C S, Jiang J C and Tao M 2011 *Solar Energy Materials and Solar Cells* **95** 3176
[7] Haegel N M, Margolis R, Buonassisi T, Feldman D, Froitzheim A, Garabedian R, Green M, Glunz S, Henning H M, Holder B, Kaizuka I, Kroposki B, Matsubara K, Niki S, Sakurai K, Schindler R A, Tumas W, Weber E R, Wilson G, Woodhouse M and Kurtz S 2017 *Science* **356** 141
[8] Ochoa M, Yang S C, Nishiwaki S, Tiwari A N and Carron R 2022 *Adv. Energy Mater.* **12** 2102800
[9] Kim G, Kim W M, Park J K, Kim D, Yu H and Jeong J H 2019 *Acs Appl. Mater. Interface* **11** 31923
[10] Ou C Y, Som S, Lu C H, Gupta K K and Chaurasiya R 2021 *J. Alloys Compd.* **881** 160377
[11] Yin G C, Brackmann V, Hoffmann V and Schmid M 2015 *Solar Energy Materials and Solar Cells* **132** 142
[12] Mansfield L M, Kanevce A, Harvey S P, Bowers K, Beall C, Glynn S and Repins I L 2018 *Progress in Photovoltaics* **26** 949
[13] Yin G C, Song M, Duan S, Manley P, Greiner D, Kaufmann C A and Schmid M 2016 *ACS Appl. Mater. Interfaces* **8** 31646
[14] Bose S, Cunha J M V, Suresh S, De Wild J, Lopes T S., Barbosa J R S, Silva R, Borme J, Fernandes P A, Vermang B and Salome P M P 2018 *Solar RRL* **2** 1800212
[15] Vermang B, Fjallstrom V, Pettersson J, Salome P and Edoff M 2013 *Solar Energy Materials and Solar Cells* **117** 505
[16] Casper P, Hunig R, Gomard G, Kiowski O, Reitz C, Lemmer U, Powalla M and Hetterich M 2016 *Physica Status Solidi-Rapid Research Letters* **10** 376
[17] Jarzembowski E, Fuhrmann B, Leipner H, Franzel W and Scheer R 2017 *Thin Solid Films* **633** 61
[18] Kotipalli R, Poncelet O, Li G, Zeng Y, Francis L A, Vermang B and Flandre D 2017 *Solar Energy* **157** 603
[19] Salome P M P, Vermang B, Ribeiro-Andrade R, Teixeira J P, Cunha J M V, Mendes M J, Haque S, Borme J, Aguas H, Fortunato E, Martins R, Gonzalez J C, Leitao J P, Fernandes P A, Edoff M and Sadewasser S 2018 *Adv. Mater. Interfaces* **5** 10

[20] Rezaei N, Isabella O, Vroon Z and Zeman M 2018 *Opt. Express* **26** A39

[21] Cunha J M V, Oliveira K, Lontchi J, Lopes T S, Curado M A, Barbosa J R S, Vinhais C, Chen W C, Borme J, Fonseca H, Gaspar J, Flandre D, Edoff M, Silva A G, Teixeira J P, Fernandes P A and Salome P M P 2021 *Solar RRL* **5** 13

[22] Lontchi J, Zhukova M, Kovacic M, Krc J, Chen W C, Edoff M, Bose S, Salome P M P, Goffard J, Cattoni A, Gouillart L, Collin S, Gusak V and Flandre D 2020 *IEEE Journal of Photovoltaics* **10** 1908

[23] Nakada T, Hirabayashi Y, Tokado T, Ohmori D and Mise T 2004 *Solar Energy* **77** 739

[24] Heinemann M D, Efimova V, Klenk R, Hoepfner B, Wollgarten M, Unold T, Schock H W and Kaufmann C A 2015 *Progress in Photovoltaics* **23** 1228

[25] Li Y, Yin G C, Gao Y, Kohler T, Lucassen J and Schmid M 2021 *Solar Energy Materials and Solar Cells* **223** 6

[26] Shin M J, Park S, Lee A, Park S J, Cho A, Kim K, Ahn S K, Park J H, Yoo J, Shin D, Jeong I, Yun J H, Gwak J and Cho J S 2021 *Appl. Surf. Sci.* **535** 9

[27] Li Y, Yin G C and Schmid M 2022 *Solar Energy Materials and Solar Cells* **234** 9

[28] Larsen J K, Simchi H, Xin P, Kim K and Shafarman W N 2014 *Appl. Phys. Lett.* **104** 033901

[29] Simchi H, Larsen J K, Kim K and Shafarman W N 2014 *IEEE Journal of Photovoltaics* **4** 1630

[30] Shin M J, Lee A, Cho A, Kim K, Ahn S K, Park J H, Yoo J, Yun J H, Gwak J, Shin D, Jeong I and Cho J S 2021 *Nano Energy* **82** 10

[31] Kim D, Shin S S, Lee S M, Cho J S, Yun J H, Lee H S and Park J H 2020 *Adv. Funct. Mater.* **30** 14

[32] Jeong W S, Lee J W, Jung S, Yun J H and Park N G 2011 *Solar Energy Materials and Solar Cells* **95** 3419

[33] Simchi H, McCandless B E, Meng T and Shafarman W N 2014 *J. Appl. Phys.* **115** 8

[34] Saifullah M, Kim K, Shahzad R, Gwak J, Cho J S, Yoo J S, Yun J H and Park J H 2018 *Solar Energy Materials and Solar Cells* **178** 29

[35] Son Y S, Yu H, Park J K, Kim W M, Ahn S Y, Choi W, Kim D and Jeong J H 2019 *J. Phys. Chem. C* **123** 1635

[36] Tu Y, Li Y, Klenk R, Yin G C and Schmid M 2022 *Progress in Photovoltaics* **30** 393

[37] Chantana J, Arai H and Minemoto T 2016 *J. Appl. Phys.* **120** 045302

[38] Hsiao K J, Liu J D, Hsieh H H and Jiang T S 2013 *Phys. Chem. Chem. Phys.* **15** 18174

[39] Zhang X F, Kobayashi M and Yamada A 2017 *ACS Appl. Mater. Interfaces* **9** 16215

[40] Li Y, Yin G C, Tu Y, Sedaghat S, Gao Y and Schmid M 2021 *ACS Appl. Energy Mater.* **7** 9

[41] Burgelman M, Nollet P and Degrave S 2000 *Thin Solid Films* **361–362** 527

[42] Abou-Ras D, Bar M, Caballero R, Gunder R, Hages C, Heinemann M D, Kaufmann C A, Krause M, Levcenko S, Mainz R, Marquez J, Nikolaeva A, Redinger A, Schafer N, Schorr S, Stange H, Unold T and Wilks R G 2018 *Solar Energy* **170** 102

[43] Stanbery B J, Abou-Ras D, Yamada A and Mansfield L 2022 *J. Phys. D: Appl. Phys.* **55** 173001

[44] Niemegeers A, Burgelman M, Herberholz R, Rau U, Hariskos D and Schock H W 1998 *Rogress in Photovoltaics: Research and Applications P* **6** 407

[45] Klenk R 2001 *Thin Solid Films* **387** 135

[46] Yin G C 2015 *Preparation of Ultra-Thin $CuIn_{1-x}Ga_xSe_2$ Solar Cells and Their Light Absorption Enhancement*, Ph.D. Dissertation (Tech497 Nische Universitaet, Berlin, Germany)